ISSN 1946-7664. MCFNS 2021
Vol. 13, Issue 1, pp. 29–35
Mathematical and Computational Forestry & Natural-Resource Sciences

AVAILABLE ONLINE AT HTTP://MCFNS.COM

Submitted: Feb. 21, 2021
Accepted: Mar. 30, 2021
Published: Mar. 30, 2021
Last Correction: Mar. 30, 2021

CORRECTING TREE COUNT BIAS FOR OBJECTS SEGMENTED FROM LIDAR POINT CLOUDS

Mike Strub[1*], Nathaniel Osborne[2]
[1] *Retired, Weyerhaeuser Company, USA.*
[2] *Rayonier Inc., USA*
[*] *Corresponding Author*

Abstract. We introduce a new statistical distribution for modeling the number of trees that fall in segmented LiDAR point clouds. Average tree count is modeled as a linear function of segment ground area, but the same methods can be used to fit more complex non-linear models. Although observed mean occurrences can be continuous, occurrences must be a non-negative integer implying the usual assumption of normal errors may not be adequate. The starting point for a new distribution is the Poisson. The Poisson is based on the premise of rare events from a large population. The probability a particular tree falls in a given point cloud segment is small and the number of segments is large, hence the Poisson distribution should be an appropriate error distribution for modeling the number of trees that fall in a point cloud segment. Deviation from the Poisson occurs as a result of the point cloud segmentation process. The purpose of segmentation is to provide segments that contain a single tree. This implies that a Poisson with deflated probability of zero occurrences and inflated probability of one occurrence is appropriate. LiDAR point cloud data on 20 stem mapped plots are used to show the utility of this approach.

Keywords: Remote sensing; forest inventory; Lambert's W; LiDAR data; Poisson Distribution.

1 Introduction

Predicting forest inventory metrics from remotely sensed data is not a new idea (Pope, 1962). However, the ability to generate and process rich data across a wide area using computers has improved recently. Light Detection and Ranging (LiDAR) data can be collected under a variety of platforms, but aerial laser scanning (ALS) appears to be the only method with applications at an industrial scale. LiDAR point clouds generated from ALS can be post-processed into tree approximate objects (Jeronimo et al., 2018). Estimating individual tree attributes from ALS point clouds is desirable over alternatives like the area based approach, as a treelist is generated that can be furnished to growth and yield systems (e.x. individual tree models or stand table projection). To the same end, unbiased estimates of forest inventory derived from LiDAR are critical to the production of long-term sustainable forest management plans. Experience with tree approximate objects from LiDAR point clouds has found large biases in tree count and derivative forest inventory estimates. Rarely is the strength of ALS to distribute a sample unbiased estimate utilized, which requires modelers to consider the nuance between training a model and correcting an estimate (Iles, 2018). With that aim, stem-mapped plots can be installed to measure and correct tree count bias (Flewelling, 2008, 2009).

The aim of this paper is to demonstrate an error distribution novel to forestry science and statistics, the zero deflated and one inflated Poisson. The zero deflated and one inflated distribution is compared to the alternative normal and Poisson error distributions. Geometric mean log-likelihood of models developed to correct biases inherent to segmented ALS point clouds are compared for each of the error distributions. A dataset of 20 stem-mapped plots is used to make the comparison. Due to our limited sample size, we forgo benchmarking multiple segmentation algorithms, but the principles demonstrated are universally applicable.

2 Methods

2.1 Data for parameterizing models Twenty stem mapped plots were installed in loblolly pine (*Pinus taeda*) and slash pine (*Pinus elliottii*) forests representa-

Table 1: Characteristics of the twenty stem mapped plots in *Pinus taeda* and *Pinus elliottii* plantations

Variable	Mean	Min	Max
Total age	19.3	15	24
Basal area (m^2/ha)	23.4	12.8	39.9
Trees per hectare	137	58.1	260.4
Dominant height (m)	17.9	14.3	22

tive of industrial forest management practices of coastal Georgia. Plots covered a wide range of stand ages and included thinned and unthinned forests (Table 1). The location of each tree, within a given plot, was established using Haglöfs Postex system (Lämås, 2010). Relative position of each tree in a given plot was referenced to a sub-meter position measured using the Trimble R1 GNSS sub-meter receiver. Plot sizes were limited to a 13.7-meter radius, after experience with the Postex system found dense vegetation limited the ability to measure larger plot sizes (Figure 1).

Figure 1: Pine plantation with vegetation limiting plot size to 13.7-meter radius using the Haglöf Postex system.

All plot measurements were taken coincident with ALS captured between January and February 2020 using a Riegl VQ-1560i sensor. The recorded pulse density was nominally 24 points per square meter, the minimum flightline overlap was 55%, and the laser footprint diameter was 0.263-meter. The maximum sensor field of view was 58.5° equivalent to the maximum scan angle of 29.25°. The horizontal and vertical accuracy was independently validated with ground control checkpoints. The vertical RMSE for height was less than 10-centimeters at the 95% confidence interval for both vegetated and non-vegetated surfaces. These accuracy statistics were certified by a professional land surveyor to meet the National Standard for Spatial Data Accuracy (NSSDA). Treetops were detected using a fixed 2-meter circular moving window to identify local maxima. Treetop detection was completed using *lidR* (Roussel et al., 2020). Tree detected points were then segmented into individual tree polygons using marker-controlled watershed segmentation in *ForestTools* (Plowright and Roussel, 2020).

Segmentation methods for LiDAR point clouds produce estimates of individual tree crowns. The aim of segmentation algorithms is to produce segments that contain a single tree. Alternatively, segments can contain no trees or multiple trees (Figure 2). A logical candidate for the statistical distribution of the number of trees per segment is the Poisson probability mass function. The Poisson distribution assumes a large number of cloud segments and a small probability that a particular tree is in any given segment. As the aim of segmentation algorithms is to have a single tree in each segment, it is likely that the number of occurrences of zero trees in the segment is deflated and the number of one tree per segment is inflated. Over the twenty stem mapped plots, 969 segments were formed. Segments crossing the boundary of a given stem mapped plot were dropped to avoid undercounting the average trees per segment. The empirical distributions of trees per segment along with the Poisson with the maximum likelihood estimate of λ equal to the mean trees per segment ($691/969 = 0.7131$) are plotted in Figure 3. The Poisson predicts fewer ones and more

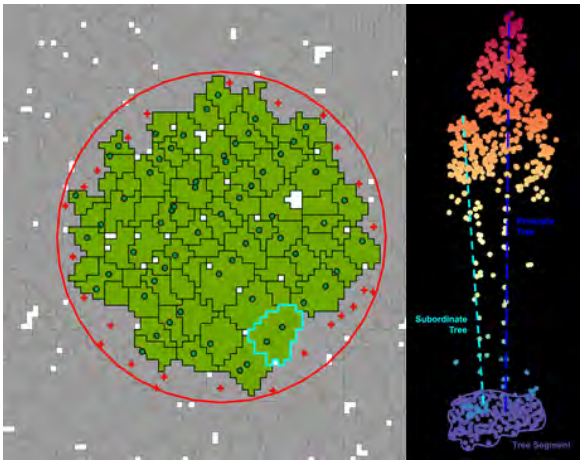

Figure 2: On the left panel a stem mapped plot demonstrates segments with inclusion of zero, one and two trees. The right panel demonstrates when a single segment includes a dominant and suppressed tree. White space indicates area between tree approximate objects.

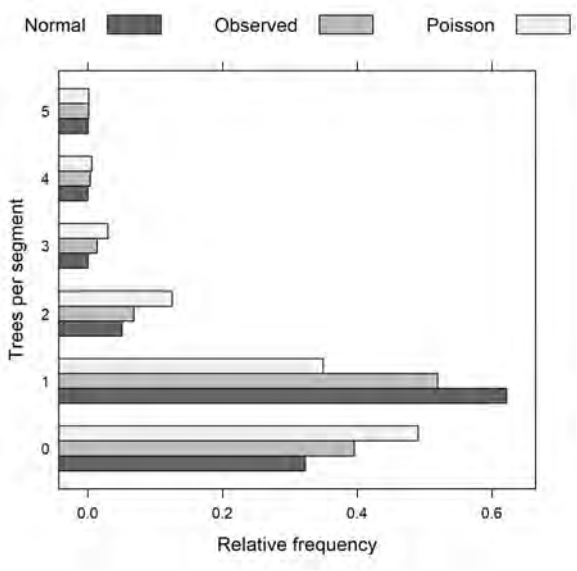

Figure 3: Relative frequency of trees per segment across 20 plots and 969 tree approximate objects with the fitted Poisson distribution with mean 0.7131 and variance (maximum likelihood definition) 0.47959.

zeros, twos and threes than observed. The Law of Large Numbers suggests the normal distribution might be a good alternative. Figure 3 shows the observed relative frequency along with the normal frequency with observed mean 0.7131 and observed variance (maximum likelihood definition) 0.47959. The normal underestimates zeros and overestimates ones. These results provide motivation for developing a method for deflating the predicted number of zeros and inflating the number of ones in the Poisson distribution. Zero inflated Poisson regression has been studied extensively, see for example Hall (2000). These regression models are not suitable for tree per segment data as the zeros are deflated rather than inflated, but we use a similar methodology to develop our model.

2.2 Zero deflated and one inflated Poisson The Poisson probability mass function is $P(X = k) = \frac{\lambda^k e^{-\lambda}}{k!}$, where k is a possible observation of trees per segment and λ is a parameter representing the mean number of trees per segment. Hence the probability of zero trees in a segment is $P(X = 0) = \frac{\lambda^0 e^{-\lambda}}{0!} = \frac{1e^{-\lambda}}{1} = e^{-\lambda}$ and the probability of a single tree in a segment is $P(X = 1) = \frac{\lambda^1 e^{-\lambda}}{1!} = \frac{\lambda e^{-\lambda}}{1} = \lambda e^{-\lambda}$. To deflate the number of zero occurrences we introduce $P(X = 0) = \pi\delta e^{-\lambda}$ and to inflate the number of single tree occurrences we assume $P(X = 1) = \theta + \delta e^{-\lambda}$. The π is a constant multiplier to reduce the number of zero occurrences and is constrained in the estimation algorithm to be between zero and one. The θ is added to the probability of one tree to increase the number of occurrences as a constant multiplier that is constrained in the estimation algorithm to be between zero and one. The δ is a multiplier added to all probabilities in the Poisson distribution to ensure probabilities sum to one, so $P(X = k > 1) = \frac{\delta\lambda^k e^{-\lambda}}{k!}$. The fact that the probabilities must sum to one implies that $\delta = \frac{1-\theta}{1+(\pi-1)e^{-\lambda}}$. A detailed proof is given in Appendix A. We also derive the expected value or mean of the new distribution, $E(X) = \theta + \frac{\lambda(1-\theta)}{[1+(\pi-1)e^{-\lambda}]}$, in the appendix. We will develop a prediction equation (either a constant or mean or a linear equation) represented by $\widehat{X}$ that will estimate $E(X)$. We make the substitution $E(X) = \widehat{X}$ and solve for $\lambda = \frac{(\widehat{X}-\theta)}{(1-\theta)} + W\left[\frac{(\widehat{X}-\theta)(\pi-1)}{(1-\theta)} e^{\frac{(\theta-\widehat{X})}{(1-\theta)}}\right]$ in the appendix and where, $W[x]$ is the Lambert W function. The Lambert W function is useful in that the solution to $x = a + be^{cx}$ is $x = a - \frac{1}{c}W\left[-bce^{ac}\right]$ (Brito et al., 2008). Finally, we use these results to derive the likelihood function for the zero deflated and one inflated Poisson. Given a set of observations x_1, x_2, …, x_n (the number of trees observed in each segment in our case) and corresponding predicted values $\widehat{X_1}$, $\widehat{X_2}$, …, $\widehat{X_n}$ the likelihood function can be developed for the linear model. For the constant or mean approach, $\widehat{X}$ is constant and the same results apply. The likelihood function is defined as $L = \prod_{i=1}^{n} P(x_i = k)$. When $x_i = 0$ we have $P(x_i = 0) = \frac{\pi(1-\theta)e^{-\lambda_i}}{1+(\pi-1)e^{-\lambda_i}}$ when $x_i = 1$ we have $P(x_i = 1) = \theta + \frac{(1-\theta)\lambda_i e^{-\lambda_i}}{1+(\pi-1)e^{-\lambda_i}}$ and when $x_i = k > 1$ we have $P(x_i = k > 1) = \frac{(1-\theta)\lambda_i^k e^{-\lambda_i}}{(1+(\pi-1)e^{-\lambda_i})k!}$, where $\lambda_i = \frac{(\widehat{X_i}-\theta)}{(1-\theta)} + W\left[\frac{(\widehat{X_i}-\theta)(\pi-1)}{(1-\theta)} e^{\frac{(\theta-\widehat{X_i})}{(1-\theta)}}\right]$. In practice the negative log likelihood is usually minimized.

3 Results

Maximum likelihood was used to fit the zero inflated Poisson, the one inflated Poisson and the zero deflated and one inflated Poisson. Two models were considered, constant $\widehat{X}$ for all i and $\widehat{X}$ varying according to a linear equation conditioned upon segment ground area, $\widehat{X} = \beta_0 + \beta_1 area$ where parameters β_0 and β_1 are the intercept and slope and the independent variable is the segment ground area. Estimates for π and θ were also obtained as part of the maximization process. Parameter estimates are given in Table 2. Figure 4 shows

Table 2: Summary statistics of maximum likelihood estimates for twenty stem mapped plots installed in *Pinus taeda* and *Pinus elliottii* plantations, with error distribution (Dist') Poisson = P, Normal = N, Zero deflated Poisson = 0P, One inflated Poisson = 1P and Zero deflated One inflated Poisson = 01P. β_0 is the intercept and β_1 is the slope of the linear prediction equation in segment ground area used to predict λ, while π is a multiplier used to deflate the Poisson probability of zero trees per segment and θ is added to the probability of one tree per segment, and $\overline{L}$ is the geometric mean likelihood for the indicated error distribution.

Dist'	$\boldsymbol{\beta_0}$	$\boldsymbol{\beta_1}$	$\boldsymbol{\pi}$	$\boldsymbol{\theta}$	$\overline{\boldsymbol{L}}$
P	0.7131	0			0.3534
P	0.0	0.1060			0.3938
N	0.7131	0			0.3496
N	0.1202	0.0882			0.4194
0P	0.7131	0	0.2640	0	0.3754
0P	0.0151	0.1050	0.0808	0	0.4543
1P	0.7131	0	1	0.2830	0.3776
1P	0.0031	0.1117	1	0.4421	0.4507
01P	0.7130	0	1	0.2830	0.3776
01P	0.0151	0.1050	0.0809	0.0	0.4543

the resulting observed and estimated relative frequency. All three distributions mimic the observed relative frequency.

Of several potential predictor variables for mean trees per segment, ground area of a given segment was shown to be particularly informative as illustrated in Figure 5. An exhaustive evaluation of the model is not provided, due to a small sample size and correspondingly limited power to test significance of alternative predictor variables. As segment ground area increases, so does the number of enveloped trees identified from stem-mapping. A linear model to predict trees per segment from ground area was fitted for each distribution. The parameter estimates along with geometric mean log likelihood are presented in Table 2. The Poisson gave the poorest fit followed by the normal distribution. The zero inflated Poisson, the one inflated Poisson and the zero deflated and one inflated Poisson all provided superior fits to the data as indicated by geometric mean likelihood over 0.45.

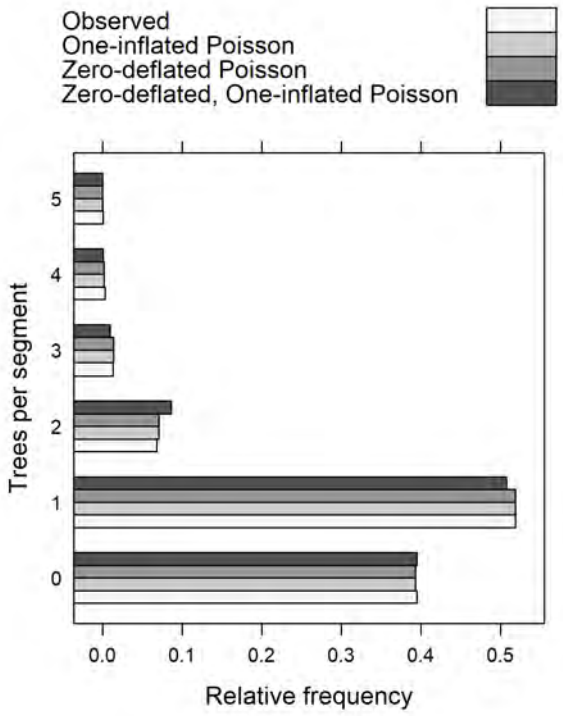

Figure 4: Relative frequency of trees per segment across 20 stem mapped plots and 969 tree approximate objects and fitted zero inflated Poisson, the one inflated Poisson and the zero-deflated and one inflated Poisson.

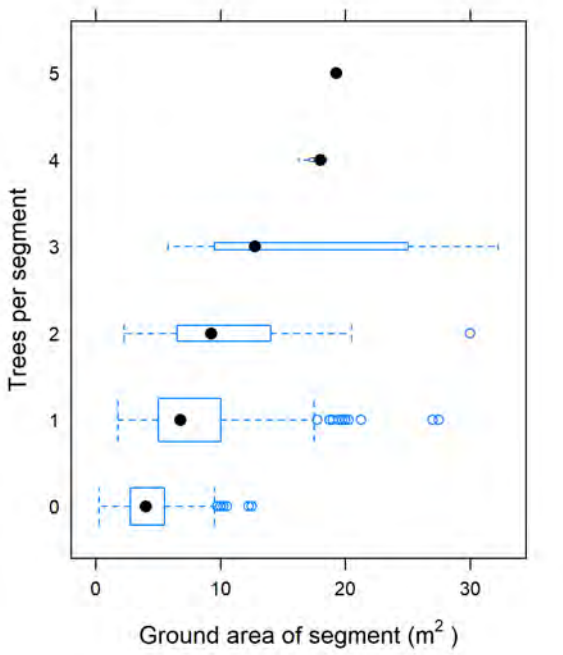

Figure 5: Relationship between trees per segment and ground area of a given segment.

4 Discussion

It is interesting to note that the most likely distribution for the intercept only single mean model is the one inflated Poisson, while the most likely distribution for the linear model is the zero deflated and one inflated Poisson. Overall, the simpler one inflated Poisson is a good choice. By setting π equal to one in the derivation of λ a simpler formula that does not involve the Lambert W can be derived, namely $\lambda = \frac{(\bar{X}-\theta)}{(1-\theta)}$. The methods presented assume linearity in the predictor variable, but results would suggest improvements could be made by imposing constraints and considering non-linearity between the response and predictor variables, as demonstrated in Figure 5. Addition of other predictor variables are likely to further enhance accuracy of the fitted models. All procedures presented are amenable to inclusion of multiple predictor variables and can be fit using *optim* in R (R Core Team (2020), Appendix B). The R program in Appendix B illustrates fitting the zero deflated one inflated Poisson, while the provided Excel file illustrates fitting the one inflated Poisson by minimizing the negative log likelihood with the Solver add-in.

5 Conclusions

Results corroborated findings from others that tree count estimates derived from segmented ALS point clouds are unlikely to identify every tree. Depending on the quality of LiDAR data, and segmentation algorithm, there may be zero inflation, deflation or other modalities. Distributions novel to forestry and statistics are given to provide modelers options for correcting these biases which are likely to require evaluation and testing specific to LiDAR collection projects. This research demonstrates a failure of segmentation to positively identify every tree and the importance of making corrections to avoid biased estimates of tree count and derivative metrics such as stand merchantable volume. Even when corrections are applied, the outcomes are designed to be regionally unbiased, suggesting that estimates at the stand or segment level will still express some degree of bias.

Acknowledgments

The authors thank Stephanie Patton, Trevor Host and Ryan Mayo of Rayonier for their assistance in preparation of data and figures. We also thank Rayonier Inc. for graciously contributing a dataset to allow other researchers to replicate and build upon these results. We sincerely appreciate the challenging and thought provoking reviews provided by Jim Flewelling, Kim Iles and an anonymous reviewer, which we believe, have significantly enhanced this article.

References

Brito, P., F. Fabiao, and A. Staubyn. 2008. Euler, lambert, and the lambert w-function today. Mathematical Scientist 33(2).

Flewelling, J. 2008. Probability models for individually segmented tree crown images in a sampling context. Proceedings of SilviLaser 2008:8th.

Flewelling, J. 2009. Forest inventory predictions from individual tree crowns: regression modeling within a sample framework. In In: McRoberts, R.E.; Reams, G.A.; Van Deusen, P.C.; McWilliams, W.H., eds. Proceedings of the eighth annual forest inventory and analysis symposium; 2006 October 16-19; Monterey, CA. Gen. Tech. Report WO-79. Washington, DC: US Department of Agriculture, Forest Service. 203-210., volume 79.

Hall, D. 2000. Zero-inflated poisson and binomial regression with random effects: a case study. Biometrics 56(4):1030–1039.

Iles, K. 2018. Are models the answer? Mathematical and Computational Forestry & Natural Resource Sciences 10(1):6. URL `http://mcfns.net/index.php/Journal/article/view/10.2`.

Jeronimo, S., V. Kane, D. Churchill, R. McGaughey, and J. Franklin. 2018. Applying lidar individual tree detection to management of structurally diverse forest landscapes. Journal of Forestry 116(4):336–346.

Lämås, T. 2010. The haglöf postex ultrasound instrument for the positioning of objects on forest sample plots. Technical Report. Umeå, Sweden, Dept. of Forest Resource Management, Arbetsrapport / Sveriges lantbruksuniversitet, Institutionen för skoglig resurshushållning och geomatik 296.

Plowright, A., and J. Roussel. 2020. Foresttools: Analyzing remotely sensed forest data. R package version 0.2.1 .

Pope, R., 1962. Constructing aerial photo volume tables. USDA Forest Service PNW Old Series Research Paper No. 49: 1-25 49.

R Core Team. 2020. R: A Language and Environment for Statistical Computing. R Foundation for Statistical Computing, Vienna, Austria. URL `https://www.R-project.org/`.

Roussel, J., D. Auty, N. Coops, P. Tompalski, T. Goodbody, A. Meador, J. Bourdon, F. de Boissieu, and A. Achim. 2020. lidr: An r package for analysis of airborne laser scanning (als) data. Remote Sensing of Environment 251:112061.

6 Appendix

Appendix A: Derivation of the zero deflated and one inflated Poisson

We use the fact that the probabilities must sum to one to solve for δ:

$$\begin{aligned}
\sum_{k=0}^{\infty} P(x=k) =& \pi\delta e^{-\lambda} + \theta + \delta\lambda e^{-\lambda} + \delta\sum_{k=2}^{\infty}\frac{\lambda^k e^{-\lambda}}{k!} \\
=& \pi\delta e^{-\lambda} + \theta + \delta\lambda e^{-\lambda} + \delta\left(1 - e^{-\lambda} - \lambda e^{-\lambda}\right) \\
=& \pi\delta e^{-\lambda} + \theta + \delta\lambda e^{-\lambda} + \delta - \delta e^{-\lambda} - \delta\lambda e^{-\lambda} \\
=& \pi\delta e^{-\lambda} + \theta + \delta - \delta e^{-\lambda} = 1 \\
\delta\left(\pi e^{-\lambda} + 1 - e^{-\lambda}\right) =& 1 - \theta \\
\delta =& \frac{1-\theta}{1 + \pi e^{-\lambda} - e^{-\lambda}} \\
=& \frac{1-\theta}{1 + (\pi - 1)\, e^{-\lambda}}
\end{aligned}$$

We next derive the expected value or mean of the new distribution.

$$\begin{aligned}
E(X) =& \sum_{k=0}^{\infty} kP(x=k) \\
=& 0\left[\frac{\pi(1-\theta)e^{-\lambda}}{1+(\pi-1)e^{-\lambda}}\right] + 1\left[\theta + \frac{(1-\theta)\lambda e^{-\lambda}}{1+(\pi-1)e^{-\lambda}}\right] + \frac{(1-\theta)}{(1+(\pi-1)e^{-\lambda})}\sum_{k=2}^{\infty}\frac{k\lambda^k e{-\lambda}}{k!} \\
=& \theta + \frac{(1-\theta)\lambda e^{-\lambda}}{1+(\pi-1)e^{-\lambda}} + \frac{\lambda(1-\theta)}{[1+(\pi-1)e^{-\lambda}]}\sum_{k=2}^{\infty}\frac{\lambda^{k-1}e^{-\lambda}}{(k-1)!} \\
=& \theta + \frac{(1-\theta)\lambda e^{-\lambda}}{1+(\pi-1)e^{-\lambda}} + \frac{\lambda(1-\theta)}{[1+(\pi-1)e^{-\lambda}]}\sum_{k=1}^{\infty}\frac{\lambda^{k}e^{-\lambda}}{k!} \\
=& \theta + \frac{(1-\theta)\lambda e^{-\lambda}}{1+(\pi-1)e^{-\lambda}} + \frac{\lambda(1-\theta)}{[1+(\pi-1)e^{-\lambda}]}(1-e^{-\lambda}) \\
=& \theta + \frac{(1-\theta)\lambda e^{-\lambda}}{1+(\pi-1)e^{-\lambda}} + \frac{\lambda(1-\theta)}{[1+(\pi-1)e^{-\lambda}]} + \frac{(1-\theta)\lambda e^{-\lambda}}{[1+(\pi-1)e^{-\lambda}]} \\
=& \theta + \frac{\lambda(1-\theta)}{[1+(\pi-1)e^{-\lambda}]}
\end{aligned}$$

We will develop a prediction equation represented by $\widehat{X}$ that will estimate $E(X)$. We make the substitution $E(X) = \widehat{X}$ and solve for λ.

$$\begin{aligned}
\widehat{X} =& \theta + \frac{\lambda(1-\theta)}{(1+(\pi-1)e^{-\lambda})} \\
\lambda =& \frac{(\widehat{X}-\theta)\left[1+(\pi-1)e^{-\lambda}\right]}{(1-\theta)} = \frac{(\widehat{X}-\theta) + (\widehat{X}-\theta)(\pi-1)e^{-\lambda}}{(1-\theta)} \\
=& \frac{(\widehat{X}-\theta)}{(1-\theta)} + \frac{(\widehat{X}-\theta)(\pi-1)}{(1-\theta)}e^{-\lambda} = \frac{(\widehat{X}-\theta)}{(1-\theta)} + W\left[\frac{(\widehat{X}-\theta)(\pi-1)}{(1-\theta)}e^{\frac{(\theta-\widehat{X})}{(1-\theta)}}\right]
\end{aligned}$$

Where $W[x]$ is the Lambert's W function. The Lambert's W is useful in that the solution to $x = a + be^{cx}$ is $x = a - \frac{1}{c}W(-bce^{ac})$.

Appendix B: R code demonstrating modifications to the Poisson distribution

```
library(lamW)
# Load data file \href{http://mcfns.net/index.php/Journal/article/view/13.3/2021.3S}{data.csv
df = read.csv("data.csv")
y = df$tps
x = df$crownarea_m

# zero deflated and one inflated Poisson
# additive inflation parameter theta greater than zero
# multiplative deflation parameter pi greater than zero
nLL.0D1I.Poisson <- function(pi,theta,est,obs){
lambda <- (est-theta)/(1-theta)+lambertW0((est-theta)*(pi-1)
*exp((theta-est)/(1-theta))/(1-theta))
delta <- (1-theta)/(1+(pi-1)*exp(-lambda))
L <- delta*lambda^obs*exp(-lambda)/factorial(obs) # Poisson adjusted for pi and theta
L.0 <- pi*L[obs==0] # deflate the zero observations
L.1 <- theta+L[obs==1] # inflate the one observations
L <- c(L.0,L.1,L[obs>1]) # other observations remain the same
return(-sum(log(L))) # return the negative log likelihood to be minimized by optim
}

# this is the function that predicts the mean trees per segment
est.freq <- function(beta,x,obs) {
est <- exp(beta[1]) + exp(beta[2]) * x
# pi must be between zero and one
pi <- 1/(1+exp(beta[3]))
# theta must be between zero and one
theta <- 1/(1+exp(beta[4]))
nLL <- nLL.0D1I.Poisson(pi,theta,est,obs)
return(nLL)
}

beta <- c(-5.7959495,-2.28,log(1/0.999-1),0.2325979)
beta <- c(log(0.12016),log(0.1115),log(1/0.001-1),log(1/0.001-1))
beta <- c(-4.2,-2.2,2.4,0.25)
beta <- c(-5.8,-2.3,4.2,0.23)
parms <- optim(beta, est.freq, x = x, obs = y)

beta <- parms$par
parms <- optim(beta, est.freq, x = x, obs = y)
beta <- parms$par
parms <- optim(beta, est.freq, x = x, obs = y)
beta <- parms$par
parms <- optim(beta, est.freq, x = x, obs = y)
intercept <- exp(parms$par[1])
slope <- exp(parms$par[2])
pi <- 1/(1+exp(parms$par[3]))
theta <- 1/(1+exp(parms$par[4]))
avg.likelihood <- exp(-parms$value/length(y))
```